

1 Perfect Sampling for Hard Spheres from Strong 2 Spatial Mixing

3 **Konrad Anand**

4 Queen Mary, University of London, UK

5 **Andreas Göbel**

6 Hasso Plattner Institute, University of Potsdam, DE

7 **Marcus Pappik**

8 Hasso Plattner Institute, University of Potsdam, DE

9 **Will Perkins**

10 School of Computer Science, Georgia Institute of Technology, USA

11 — Abstract —

12 We provide a perfect sampling algorithm for the hard-sphere model on subsets of \mathbb{R}^d with expected
13 running time linear in the volume under the assumption of strong spatial mixing. A large number of
14 perfect and approximate sampling algorithms have been devised to sample from the hard-sphere
15 model, and our perfect sampling algorithm is efficient for a range of parameters for which only
16 efficient approximate samplers were previously known and is faster than these known approximate
17 approaches. Our methods also extend to the more general setting of Gibbs point processes interacting
18 via finite-range, repulsive potentials.

19 **2012 ACM Subject Classification** Theory of computation → Randomness, geometry and discrete
20 structures

21 **Keywords and phrases** perfect sampling, hard-sphere model, Gibbs point processes

22 **Digital Object Identifier** 10.4230/LIPIcs.APPROX/RANDOM.2023.38

23 **Category** RANDOM

24 **Related Version** *Full Version*: <https://arxiv.org/abs/2305.02450> [3]

25 **Funding** *Konrad Anand*: funded by a studentship from Queen Mary, University of London
26 *Andreas Göbel*: funded by the project PAGES (project No. 467516565) of the German Research
27 Foundation (DFG)

28 *Marcus Pappik*: funded by the HPI Research School on Data Science and Engineering

29 *Will Perkins*: supported in part by NSF grant DMS-2309958

30 **Acknowledgements** We thank Mark Jerrum for very helpful discussions on this topic.

31 **1** Introduction

32 Gibbs point processes, or classical gases, are mathematical models of interacting particles. In
33 statistical physics they are used to model gases, fluids, and crystals, while in other fields they
34 are used to model spatial phenomena such as the growth of trees in a forest, the distribution
35 of stars in the universe, or the location of cities on a map (see e.g. [68, 59, 73, 12]).

36 Perhaps the longest and most intensively studied Gibbs point process is the hard-sphere
37 model: a model of a gas in which the only interaction between particles is a hard-core
38 exclusion in a given radius around each particle. That is, it is a model of a random packing
39 of equal-sized spheres. Despite the simplicity of its definition, the hard-sphere model is
40 expected to exhibit the qualitative behavior of a real gas [2], and in particular exhibits
41 gas, liquid, and solid phases, thus giving evidence for the hypothesis, dating back to at



© Konrad Anand, Andreas Göbel, Marcus Pappik and Will Perkins;
licensed under Creative Commons License CC-BY 4.0

Approximation, Randomization, and Combinatorial Optimization. Algorithms and Techniques
(APPROX/RANDOM 2023).

Editors: Nicole Megow and Adam D. Smith; Article No. 38; pp. 38:1–38:18



Leibniz International Proceedings in Informatics
Schloss Dagstuhl – Leibniz-Zentrum für Informatik, Dagstuhl Publishing, Germany

42 least Boltzmann, that the macroscopic properties of a gas or fluid are determined by its
 43 microscopic interactions. This rich behavior exhibited by the hard-sphere model is very
 44 difficult to analyze rigorously, and the most fundamental questions about phase transitions
 45 in this model are open mathematical problems [68, 50].

46 In studying the hard-sphere model (or Gibbs point processes more generally), a funda-
 47 mental task is to sample from the model. Sampling is used to estimate statistics, observe
 48 evidence of phase transitions, and perform statistical tests on data. A wide variety of meth-
 49 ods have been proposed to sample from these distributions; for instance, the Markov chain
 50 Monte Carlo (MCMC) method was first proposed by Metropolis, Rosenbluth, Rosenbluth,
 51 Teller, and Teller [53] to sample from the two-dimensional hard-sphere model. Understand-
 52 ing sampling methods for point processes in theory and in practice is a major area of
 53 study [58, 59, 16, 39, 47], and advances in sampling techniques have led to advances in the
 54 understanding of the physics of these models [53, 2, 50, 7, 6, 16].

55 In this paper we will be concerned with provably efficient sampling from the hard-sphere
 56 model. Rigorous guarantees for sampling algorithms come in several different varieties. One
 57 question is what notion of ‘efficient’ to use; another is what guarantee we insist on for the
 58 output. In this paper we will provide an efficient sampling algorithm under the strictest
 59 possible terms with respect to both running time and accuracy of the output: a linear-time,
 60 *perfect* sampling algorithm.

61 For simplicity we focus on sampling from the hard-sphere model defined on finite boxes
 62 in \mathbb{R}^d . For fixed parameter values of the model, the typical number of points appearing in
 63 such a region is linear in the volume, and so any sampling algorithm will require at least this
 64 much time.

65 As for guarantees on the output, there are two main types of guarantees. The first type is
 66 an *approximate sampler*: the output of such an algorithm must be distributed within ε total
 67 variation distance of the desired target distribution. Perhaps the main approach to efficient
 68 sampling from distributions normalized by intractable normalizing constants is the MCMC
 69 method. In this approach, one devises a Markov chain with the target distribution as the
 70 stationary distribution and runs a given number steps of the chain from a chosen starting
 71 configuration; if the number of steps is at least the ε -mixing time, then the final state has
 72 distribution within ε total variation distance of the target [42, 65, 13]. In general, however,
 73 computing or bounding the mixing time can be a very challenging problem.

74 The second type of guarantee is that of a *perfect sampler* [63]. Such an algorithm has a
 75 running time that is random, but the distribution of the output is guaranteed to be *exactly*
 76 that of the target distribution. The main advantage of perfect sampling algorithms – and
 77 the primary reason they are studied and used in practice – is that one need not prove a
 78 theorem or understand the mixing time of a Markov chain to run the algorithm and get
 79 an accurate sample; one can simply run the algorithm and know that the output has the
 80 correct distribution. The drawback is that the running time may be very large, depending on
 81 the specific algorithm and on the parameter regime. Some naive sampling methods such as
 82 rejection sampling return perfect samples but are inefficient on large instances (exponential
 83 expected running time in the volume). The breakthrough of Propp and Wilson in introducing
 84 ‘coupling from the past’ [63, 64] was to devise a procedure for using a Markov chain transition
 85 matrix to design perfect sampling algorithms which, under some conditions, could run in time
 86 polylogarithmic in the size of a discrete state space (polynomial-time in the size of the graph
 87 of a spin system), matching the efficiency of fast mixing Markov chains which only return
 88 approximate samples (see also [5, 49] for precedents in perfect sampling). The work of Propp
 89 and Wilson led to numerous constructions of perfect sampling algorithms for problems with

90 both discrete and continuous state spaces including [17, 27, 45, 60, 28, 21, 46, 58, 23]. Notably,
 91 many of the first applications of Propp and Wilson’s technique were in designing perfect
 92 sampling algorithms for Gibbs point processes (though often without rigorous guarantees on
 93 the efficiency of the algorithms).

94 Perfect sampling continues to be a very active area of research today, with a special focus
 95 on improving the range of parameters for which perfect sampling algorithms can (provably)
 96 run in expected linear or polynomial time [9, 40, 30]

97 In this paper we design a perfect sampling algorithm for the hard-sphere model (and
 98 Gibbs point processes interacting with a finite-range, repulsive pair potential more generally)
 99 that is guaranteed to run in linear expected time for activity parameters up to the best
 100 known bound for efficient approximate sampling via MCMC.

101 What is this bound and how do we design the algorithm? One central theme in the
 102 analysis of discrete spin systems is the relationship between spatial mixing (correlation decay
 103 properties) and temporal mixing (mixing times of Markov chains) [35, 1, 72, 52, 15]. At
 104 a high level, these works show that for discrete lattice systems a strong correlation decay
 105 property (*strong spatial mixing*) implies a near-optimal convergence rate for local-update
 106 Markov chains like the Glauber dynamics. Recently it has been showed that strong spatial
 107 mixing in a discrete lattice model also implies the existence of efficient *perfect* sampling
 108 algorithms [18, 4]. In parallel, there has been work establishing the connection between
 109 strong spatial mixing and optimal temporal mixing for Markov chains in the setting of the
 110 hard-sphere model and Gibbs point processes [33, 55, 56]. At a high level, our aim is to
 111 combine these threads to show that strong spatial mixing for Gibbs point processes implies
 112 the existence of an efficient perfect sampler. One challenge is that the approaches of [18, 4]
 113 are inherently discrete in that key steps of the algorithms involve enumerating over all
 114 possible configurations in a subregion, something that is not possible in the continuum. To
 115 overcome this we make essential use of Bernoulli factories – a method for perfect simulation
 116 of a coin flip with a bias $f(p)$ given access to coin flips of bias p . Bernoulli factories have
 117 recently been used in perfect sampling algorithms for solutions to constraint satisfaction
 118 problems in [31, 32].

119 1.1 The hard-sphere model, strong spatial mixing, and perfect sampling

120 The hard-sphere model is defined on a bounded, measurable subset Λ of \mathbb{R}^d with an activity
 121 parameter $\lambda \geq 0$ that governs the density of the model and a parameter $r > 0$ that governs
 122 the range of interaction (though by re-scaling there is really only one meaningful parameter,
 123 and we could take $r = 1$ without loss of generality). In words, the hard-sphere model is the
 124 distribution of finite point sets in Λ obtained by taking a Poisson point process of activity λ
 125 on Λ and conditioning on the event that all pairs of points are at distance at least r from
 126 each other; in other words, on the event that spheres of radius $r/2$ centered at the given
 127 points form a sphere packing.

128 We can equivalently define the model more explicitly, and in doing so, introduce objects
 129 and notation we work with throughout the paper. To begin, let \mathcal{N}_Λ be the set of all finite point
 130 sets in Λ . Each point set $\eta \in \mathcal{N}_\Lambda$ represents a particle configuration in Λ . Write $\mathfrak{R}_\Lambda \subseteq 2^{\mathcal{N}_\Lambda}$
 131 for the σ -field generated by the maps $\{\mathcal{N}_\Lambda \rightarrow \mathbb{N}_0, \eta \mapsto |\eta \cap B| \mid B \subseteq \Lambda \text{ Borel-measurable}\}$.
 132 The hard-sphere model (or in fact any Gibbs point process) is a probability measure μ_λ on
 133 the space $(\mathcal{N}_\Lambda, \mathfrak{R}_\Lambda)$.

134 Define for every $x_1, \dots, x_k \in \mathbb{R}^d$ the indicator that the points are centers of non-

38:4 Perfect Sampling for Hard Spheres from Strong Spatial Mixing

135 overlapping spheres of radius $r/2$; that is,

$$136 \quad D(x_1, \dots, x_k) = \prod_{\{i,j\} \in \binom{[k]}{2}} \mathbb{1}_{\text{dist}(x_i, x_j) \geq r}.$$

137
138 Then define the partition function

$$139 \quad Z_\Lambda(\lambda) = \sum_{k \geq 0} \frac{\lambda^k}{k!} \int_{\Lambda^k} D(x_1, \dots, x_k) dx_1 \dots dx_k.$$

140 For an event $A \in \mathfrak{R}_\Lambda$, the hard-sphere model assigns the probability

$$141 \quad \mu_\lambda(A) = \frac{1}{Z_\Lambda(\lambda)} \sum_{k \geq 0} \frac{\lambda^k}{k!} \int_{\Lambda^k} \mathbb{1}_{\{x_1, \dots, x_k\} \in A} D(x_1, \dots, x_k) dx_1 \dots dx_k. \quad (1)$$

142 A very useful generalization of this model is to allow for a non-constant (but measurable)
143 activity function $\lambda : \Lambda \rightarrow [0, \infty)$. Here the model is a Poisson process with inhomogenous
144 activity λ conditioned on the points forming the centers of a sphere packing; the partition
145 function is now

$$146 \quad Z_\Lambda(\lambda) = \sum_{k \geq 0} \frac{1}{k!} \int_{\Lambda^k} \prod_{i=1}^k \lambda(x_i) D(x_1, \dots, x_k) dx_1 \dots dx_k$$

147 and the measure μ_λ is defined analogously to (1). This generalization allows modeling of
148 non-homogenous spaces and generalizes the concept of imposing boundary conditions on the
149 model. To see this, suppose we fix a particle configuration $\eta \in \mathcal{N}_\Lambda$ as boundary conditions.
150 Additional points are forbidden within the balls of radius r around each point $x \in \eta$; we can
151 implement the distribution of additional points by considering the measure μ_λ with $\lambda(y) = 0$
152 if $\text{dist}(y, x) < r$ for some $x \in \eta$; and $\lambda(y) = \lambda$ otherwise. We denote the resulting activity
153 function by λ by λ_η . Further, we can use this generalization to restrict a point process to
154 only place points in a subregion $\Lambda' \subseteq \Lambda$ by considering the measure $\mu_{\lambda \mathbb{1}_{\Lambda'}}$ with activity
155 function $\lambda \mathbb{1}_{\Lambda'} : x \mapsto \lambda \mathbb{1}_{x \in \Lambda'}$. Of course the generalization to measurable activity functions is
156 much more general than this, and activity functions λ need not be realizable by boundary
157 conditions or restriction to a subregion, nor take only two values.

158 This generalization to activity functions is crucial for defining *strong spatial mixing*, the
159 condition under which we can guarantee the efficiency of our perfect sampling algorithm.

160 To define the concept of strong spatial mixing we consider projections of the measure μ_λ
161 to subregions $\Lambda' \subseteq \Lambda$. We write $\mu_\lambda[\Lambda']$ for the probability measure on $(\mathcal{N}_{\Lambda'}, \mathfrak{R}_{\Lambda'})$ induced
162 by μ_λ (we make this definition formal in Section 3). We can impose two distinct boundary
163 conditions on Λ' by choosing two different activity functions λ, λ' . Strong spatial mixing
164 asserts that the distributions $\mu_\lambda[\Lambda'], \mu_{\lambda'}[\Lambda']$ are close in total variation when λ, λ' differ only
165 on points far from Λ' ; i.e., when $\text{dist}(\Lambda', \text{supp}(\lambda - \lambda'))$ is large (as $\text{supp}(\lambda - \lambda')$ is the set of
166 points at which the two activity functions disagree).

167 Writing $|\Lambda'|$ for the volume of Λ' , strong spatial mixing with exponential decay is defined
168 as follows.

169 ► **Definition 1.1.** *Given $a, b \in \mathbb{R}_{>0}$, the hard-sphere model on \mathbb{R}^d exhibits **(a, b)-strong**
170 **spatial mixing** up to $\lambda \in \mathbb{R}_{>0}$ if for all bounded measurable $\Lambda \subset \mathbb{R}^d$ the following holds: For
171 all measurable $\Lambda' \subseteq \Lambda$ and all activity functions $\lambda, \lambda' \leq \lambda$ it holds that*

$$172 \quad d_{TV}(\mu_\lambda[\Lambda'], \mu_{\lambda'}[\Lambda']) \leq a |\Lambda'| e^{-b \cdot \text{dist}(\Lambda', \text{supp}(\lambda - \lambda'))},$$

173 where $d_{TV}(\cdot, \cdot)$ denotes total variation distance.

174 This definition of strong spatial mixing comes from [56], which in turn adapted similar
 175 notions from discrete spin systems [15, 74]. Strong spatial mixing has proved to be an
 176 essential definition in the analysis, both probabilistic and algorithmic, of spin systems on
 177 graphs, and many recent works are focused on either proving strong spatial mixing for a
 178 particular model, range of parameters, and class of graphs (e.g. [74, 22, 51, 69, 66, 10]) or
 179 deriving consequences of strong spatial mixing (e.g. [70, 19, 48, 18, 4]).

180 Our main result is a linear expected-time perfect sampling algorithm for the hard-sphere
 181 model under the assumption of strong spatial mixing.

182 ► **Theorem 1.2.** *There is a perfect sampling algorithm for the hard-sphere model on finite*
 183 *boxes $\Lambda \subset \mathbb{R}^d$ with the property that if the hard-sphere model exhibits (a, b) -strong spatial*
 184 *mixing up to λ , then the expected running time of the algorithm at activity λ is $O(|\Lambda|)$, where*
 185 *the implied constant is a function of a, b , and λ .*

186 In particular, one can run the algorithm for any value of λ (without knowing whether
 187 or not strong spatial mixing holds) and the algorithm will terminate in finite time with an
 188 output distributed exactly as μ_λ ; under the assumption of strong spatial mixing the expected
 189 running time is guaranteed to be linear in the volume.

190 Using bounds from [56] on strong spatial mixing in the hard-sphere model, we obtain the
 191 following explicit bounds on the activities for which the algorithm is efficient.

192 ► **Corollary 1.3.** *The above perfect sampling algorithm runs in expected time $O(|\Lambda|)$ when*
 193 *$\lambda < \frac{e}{v_d(r)}$, where $v_d(r)$ is the volume of the ball of radius r in \mathbb{R}^d .*

194 In comparison, near-linear time MCMC-based approximate samplers were given in [56]
 195 for the same range of parameters (following results for more restricted ranges in [43, 33]).
 196 For perfect sampling from the hard-sphere model, linear expected time algorithms were given
 197 in [36, 25] for more restrictive ranges of parameters.

198 1.2 Gibbs point processes with finite-range repulsive potentials

199 We now give a closely related result in the more general setting of Gibbs point processes
 200 interacting via finite-range, repulsive pair potentials.

201 Gibbs point processes are defined via a density against an underlying Poisson point
 202 process. In general, this density is the exponential of (the negative of) an energy function on
 203 point sets that captures the interactions between points. In many of the most studied cases,
 204 this energy function takes a special form: it is the sum of potentials over pairs of points in a
 205 configuration.

206 A *pair potential* is a measurable symmetric function $\phi : \mathbb{R}^d \times \mathbb{R}^d \rightarrow \mathbb{R} \cup \{\infty\}$. For a
 207 bounded, measurable activity function λ on Λ the Gibbs point process with pair potential ϕ
 208 on Λ is defined via the partition function

$$209 \quad Z_\Lambda(\lambda) = \sum_{k \geq 0} \frac{1}{k!} \int_{\Lambda^k} \left(\prod_{i \in [k]} \lambda(x_i) \right) e^{-H(x_1, \dots, x_k)} dx_1 \dots dx_k$$

210 where

$$211 \quad H(x_1, \dots, x_k) = \sum_{\{i, j\} \in \binom{[k]}{2}} \phi(x_i, x_j).$$

212 Again the corresponding probability measure μ_λ is obtained as in (1). A pair potential
 213 ϕ is *repulsive* if $\phi(x, y) \geq 0$ for all x, y . It is of *finite-range* if there exists $r \geq 0$ so that

214 $\phi(x, y) = 0$ whenever $\text{dist}(x, y) > r$. As with the hard-sphere model, we can use the
 215 activity function to encode the influence of boundary conditions by defining the activity
 216 function $\lambda_\eta : y \mapsto \lambda e^{-\sum_{x \in \eta} \phi(x, y)}$ for any activity $\lambda \in [0, \infty)$ and particle configuration
 217 $\eta \in \mathcal{N}_\Lambda$. Moreover, strong spatial mixing for a Gibbs point process is defined exactly as in
 218 Definition 1.1.

219 The hard-sphere model is one example of a model interacting via a finite-range, repulsive
 220 pair potential; it is obtained by letting $\phi(x, y)$ take the value $+\infty$ if $\text{dist}(x, y) \leq r$ and 0
 221 otherwise. The Strauss process [71, 44] is another such example.

222 Our next result is a near-linear expected time perfect sampling algorithm for Gibbs point
 223 processes interacting via finite-range, repulsive potentials under the assumption of strong
 224 spatial mixing.

225 ► **Theorem 1.4.** *Suppose ϕ is a finite-range, repulsive potential on \mathbb{R}^d and suppose ϕ exhibits*
 226 *(a, b) -strong spatial mixing up to λ for some constants $a, b > 0$. Then there is a perfect*
 227 *sampling algorithm for the Gibbs point process defined by ϕ and activity functions bounded*
 228 *by λ on boxes Λ in \mathbb{R}^d with expected running time $O(|\Lambda| \log^{O(1)} |\Lambda|)$.*

229 One difference between this algorithm and the hard-sphere algorithm of Theorem 1.2 is
 230 that this algorithm needs knowledge of the constants a, b in the assumption of strong spatial
 231 mixing, whereas the hard-sphere algorithm does not.

232 Using the results of [56], we can get explicit bounds for the existence of efficient perfect
 233 sampling algorithms in terms of the *temperedness constant* of the potential defined by

$$234 \quad C_\phi := \sup_{x \in \mathbb{R}^d} \int_{\mathbb{R}^d} |1 - e^{-\phi(x, y)}| dy. \quad (2)$$

235 Under the assumption that ϕ is repulsive and of finite range r , we have $0 \leq C_\phi \leq v_d(r)$.

236 ► **Corollary 1.5.** *The above perfect sampling algorithm runs in expected time $O(|\Lambda| \log^{O(1)} |\Lambda|)$*
 237 *when $\lambda < \frac{e}{C_\phi}$.*

238 ► **Remark 1.6.** In fact, using the results of Michelen and Perkins [54], one can push the bound
 239 for strong spatial mixing up to e/Δ_ϕ , where $\Delta_\phi \leq C_\phi$ is the *potential-weighted connective*
 240 *constant* defined therein; our perfect sampling algorithm is efficient up to that point.

241 1.3 Related work and future directions

242 Related work

243 In recent years there has been a moderate flurry of activity around proving rigorous results
 244 for Gibbs point processes in both the setting of statistical physics and probability theory
 245 and in the setting of provably efficient sampling algorithms.

246 Work on provably efficient approximate sampling methods for the hard-sphere model
 247 begins with the seminal paper of Kannan, Mahoney, and Montenegro [43], who used techniques
 248 from the analysis of discrete spin systems to prove mixing time bounds for Markov chains
 249 for the hard-sphere model. Improvements to the range of parameters for which fast mixing
 250 holds came in [29, 33], before Michelen and Perkins proved the bound $e/v_d(r)$ in [56], which
 251 we match with a perfect sampling algorithm in Corollary 1.3.

252 Perfect sampling algorithms for the hard sphere model have been considered in [27, 46,
 253 21, 25, 38]. In terms of rigorous guarantees of efficiency, Huber proved a bound of $2/v_d(r)$
 254 for a near-linear expected time perfect sampler in [36]. The perfect sampling algorithm of

255 Guo and Jerrum in [25] does not match this bound, but the algorithm, based on ‘partial
 256 rejection sampling’ [26] is novel and particularly simple. Several of these approaches also
 257 apply for finite-range, repulsive potentials or can be extended to that setting (e.g. [57]).

258 In parallel, there has been much work on proving bounds on the range of activities
 259 for which no phase transition can occur in the hard-sphere model; and, in recent years in
 260 particular, the techniques used have close connections to algorithms and the study of Markov
 261 chains. The classic approach to proving absence of phase transition is by proving convergence
 262 of the cluster expansion; the original bound here is $1/(ev_d(r))$ due to Groeneveld [24]. In small
 263 dimensions (most significantly in dimension 2) improvements to the radius of convergence
 264 can be obtained [20]. On the other hand, this approach is inherently limited by the presence
 265 of non-physical singularities on the negative real axis. Alternative approaches avoiding
 266 this obstruction include using the equivalence of spatial and temporal mixing [33, 56]; or
 267 disagreement percolation [11, 34, 8]. The best current bound for absence of phase transition
 268 for the hard-sphere model and for repulsive pair potentials is the bound of e/C_ϕ (and e/Δ_ϕ)
 269 obtained by Michelen and Perkins [55, 56, 54]. Theorem 1.4 brings the bound for efficient
 270 perfect sampling up to this bound.

271 On a technical level, the most relevant past work is [18], in which the authors prove
 272 that for discrete spin systems, strong spatial mixing and subexponential volume growth of a
 273 sequence of graphs imply the existence of an efficient perfect sampling algorithm. We take
 274 their approach as a starting point but need new ideas to replace their exhaustive enumeration
 275 of configurations.

276 A key step in our algorithm is the use of a Bernoulli factory to implement a Bayes
 277 filter. Bernoulli factories are algorithms by which a Bernoulli random variable with success
 278 probability $f(p)$ can be simulated (perfectly) by an algorithm with access to independent
 279 Bernoulli p random variables, where the algorithm does not know the value p . Whether a
 280 Bernoulli factory exists (and how efficient it can be) depends on the function $f(\cdot)$ and a
 281 priori bounds on the possible values p . Bernoulli factories have been studied in [61, 37, 14]
 282 and recently used in the design of perfect sampling algorithms for CSP solutions in [31, 32].

283 Future directions

284 There are a number of extensions and improvements to these results one could pursue.
 285 Perhaps most straightforward would be to relax the notion of strong spatial mixing from
 286 exponential decay to decay faster than the volume growth of \mathbb{R}^d and to extend the results
 287 to repulsive potentials of unbounded range but finite temperedness constant C_ϕ . Moreover,
 288 it would be nice to upgrade the guarantees of the algorithm in Theorem 1.4 to that of
 289 Theorem 1.2: that the algorithm does not need prior knowledge of the strong spatial mixing
 290 constants a, b to run correctly.

291 An ambitious and exciting direction would be to remove the assumption of a repulsive
 292 potential and find efficient perfect sampling algorithms for the class of *stable* potentials (see
 293 e.g. [62, 67, 68] for a definition). A stable potential is repulsive at short ranges but can
 294 include a weak attractive part; such potentials include the physically realistic Lennard-Jones
 295 potential among others [75]. This would require some very new ideas, as much of the
 296 recent probabilistic and algorithmic work on Gibbs point processes (e.g. [55, 56, 8, 54]) has
 297 used repulsiveness as an essential ingredient (for one, repulsiveness of the potential implies
 298 stochastic domination by the underlying Poisson point process). As a notable exception, a
 299 deterministic approximation algorithm for partition functions of finite-range stable potentials
 300 based on cluster expansion was recently proposed in [41].

301 **1.4 Outline of the paper**

302 In Section 2, we describe the high-level idea and intuition behind the algorithm. In Section 3
 303 we introduce some notation and present some preliminary results that we will use throughout
 304 the paper. In Section 4 we present the algorithm that we will apply to both hard spheres
 305 and more general processes, and we state the main theorems and lemmas that we use for
 306 proving Theorem 1.2. The more general setting of bounded-range repulsive potentials (i.e.,
 307 Theorem 1.4) can be found in the full version of the paper [3]. Intermediate steps and proves
 308 are omitted and can be found in the full version as well.

309 **2 Intuitive idea behind the algorithm**

310 Our algorithm is an adaptation to continuum models of the work by Feng, Guo, and Yin [18]
 311 on perfect sampling from discrete spin systems. We mimic their setting of a spin system on
 312 a graph $G = (V, E)$ by putting a graphical structure on sub-regions of our continuous space.

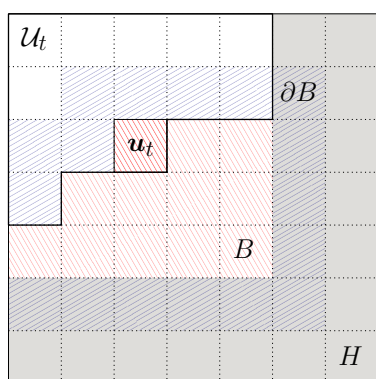
313 Let $\Lambda = [0, L]^d \subset \mathbb{R}^d$ be the region considered, $\lambda > 0$ the activity, and let ϕ be a repulsive
 314 potential of range $r > 0$. We subdivide Λ into $(\Lambda_{\mathbf{v}})_{\mathbf{v} \in \mathcal{V}}$, a set of smaller boxes of side length
 315 r indexed by vertices of a graph: each box corresponds to a vertex and boxes are connected
 316 if they are within r of each other, i.e., particles in the boxes can interact directly through the
 317 potential ϕ . We fix the index set for the boxes to be $\mathcal{V} \subset \mathbb{N}_0^d$, where each $\mathbf{v} \in \mathcal{V}$ corresponds
 318 to the box $\Lambda_{\mathbf{v}} = [v_1 r, (v_1 + 1)r) \times \cdots \times [v_d r, (v_d + 1)r)$. We extend this notation to sets of
 319 indices $S \subseteq \mathcal{V}$ by setting $\Lambda_S = \bigcup_{\mathbf{v} \in S} \Lambda_{\mathbf{v}}$. Further, we denote by $\mathbb{B}_k(\mathbf{v})$ the set of indices
 320 $\mathbf{w} \in \mathcal{V}$ with $\|\mathbf{v} - \mathbf{w}\|_{\infty} \leq k$. To shorten notation, we write $\partial S = (\bigcup_{\mathbf{v} \in S} \mathbb{B}_1(\mathbf{v})) \setminus S$ for the
 321 outer boundary of a set of boxes indexed by $S \subseteq \mathcal{V}$.

322 Our algorithm runs iteratively, keeping track of two random variables: a point config-
 323 uration $X_t \in \mathcal{N}_{\Lambda}$ with $X_0 = \emptyset$, and a set of ‘incorrect’ boxes $\mathcal{U}_t \subseteq \mathcal{V}$ with $\mathcal{U}_0 = \mathcal{V}$. With
 324 each iteration t we maintain the following *invariant*: the partial configuration $X_t \cap (\Lambda_{\mathcal{U}_t})^c$
 325 is distributed according to the projection of μ_{λ} to $(\Lambda_{\mathcal{U}_t})^c$ under the boundary condition
 326 $X_t \cap \Lambda_{\mathcal{U}_t}$. It follows that X_t is distributed according to μ_{λ} once we reach the state $\mathcal{U}_t = \emptyset$.

327 We proceed by sketching an iteration of the algorithm. An example for the involved
 328 subregions is given in Figure 1. Each iteration runs as follows:

- 329 1. We choose $\mathbf{u}_t \in \mathcal{U}_t$ uniformly at random and attempt to ‘repair’ it by updating X_t on a
 330 neighborhood of boxes $B = \{\mathbf{u}_t\} \cup (\mathbb{B}_{\ell}(\mathbf{u}_t) \setminus \mathcal{U}_t)$ for some *update radius* $\ell \in \mathbb{N}$.
- 331 2. We sample a Bayes filter F_t (i.e., a Bernoulli random variable) with probability depending
 332 on the potential ϕ , the activity λ , and the current point configuration X_t on $\Lambda_{\mathbf{u}_t}$ and
 333 $\Lambda_{\partial B}$.
- 334 3. a) If $F_t = 1$, we set $\mathcal{U}_{t+1} = \mathcal{U}_t \setminus \{\mathbf{u}_t\}$ and we get X_{t+1} by updating X_t on Λ_B according
 335 to a projection of μ_{λ} conditioned on the boundary configuration $X_t \cap (\Lambda_B)^c$.
- 336 b) If $F_t = 0$, the configuration is unchanged and we add the boundary boxes to our
 337 ‘incorrect’ list, i.e., $X_{t+1} = X_t$ and $\mathcal{U}_{t+1} = \mathcal{U}_t \cup \partial B$.

338 We use the Bayes filter, as in [18], to remove bias from the resulting distribution. To
 339 give some intuition for its role, suppose we run a naive version of the algorithm where we
 340 always update X_t on Λ_B as in step 3.a) above. Assuming the desired invariant holds after
 341 t iterations, this naive algorithm gives a bias to the distribution of X_{t+1} proportional to
 342 $\frac{Z_{\Lambda_B \setminus \{\mathbf{u}_t\}}(\lambda_{X_t \cap \Lambda_{\partial B} \cup \{\mathbf{u}_t\}})}{Z_{\Lambda_B}(\lambda_{X_t \cap \Lambda_{\partial B}})}$. We choose the Bayes filter such that, conditioned on $F_t = 1$, the



■ **Figure 1** The box-shaped region $\Lambda \subset \mathbb{R}^2$ is divided into boxes of side length r (dotted lines). The boxes \mathcal{U}_t are bordered by bold black lines. For \mathbf{u}_t as given and update radius $\ell = 2$, the corresponding set B of boxes to be updated is indicated by the red hatched area (falling left to right). Its boundary boxes ∂B are shown as blue hatched area (rising left to right). The boxes in $H = (\mathcal{U}_t \cup B)^c$ are shown with gray background.

343 bias term gets canceled. This suggests the choice

$$344 \quad \mathbb{P}[F_t = 1 \mid X_t, \mathcal{U}_t, \mathbf{u}_t] = C(\mathcal{U}_t, \mathbf{u}_t, X_t) \cdot \frac{Z_{\Lambda_B}(\lambda_{X_t \cap \Lambda_{\partial B}})}{Z_{\Lambda_B \setminus \{\mathbf{u}_t\}}(\lambda_{X_t \cap \Lambda_{\partial B \cup \{\mathbf{u}_t\}})}, \quad (3)$$

345 where the choice $C(\mathcal{U}_t, \mathbf{u}_t, X_t)$ serves three main purposes.

346 First, it must guarantee that the right-hand side of (3) is a probability. To achieve this
 347 we need, for $H = (\mathcal{U}_t \cup B)^c$ and almost all realizations of X_t, \mathcal{U}_t and \mathbf{u}_t , that

$$348 \quad C(\mathcal{U}_t, \mathbf{u}_t, X_t) \leq \inf_{\xi \in \mathcal{N}_{\Lambda_H}} \frac{Z_{\Lambda_B \setminus \{\mathbf{u}_t\}}(\lambda_{\xi \cup (X_t \cap \Lambda_{\mathcal{U}_t})})}{Z_{\Lambda_B}(\lambda_{\xi \cup (X_t \cap \Lambda_{\mathcal{U}_t \setminus \{\mathbf{u}_t\}})})}. \quad (4)$$

349 Second, $C(\mathcal{U}_t, \mathbf{u}_t, X_t)$ must introduce no new bias. Carrying out the calculations, it can be
 350 seen that this is guaranteed if $C(\mathcal{U}_t, \mathbf{u}_t, X_t)$ only depends on $X_t \cap \Lambda_{\mathcal{U}_t}$. Finally, it must ensure
 351 that the algorithm terminates almost surely. It suffices to ensure $C(\mathcal{U}_t, \mathbf{u}_t, X_t)$ is uniformly
 352 bounded away from 0 for almost all realizations of X_t , implying that the same holds for the
 353 right-hand side of (3). We refer to a function $C(\cdot)$ satisfying these requirements as a *Bayes*
 354 *filter correction*.

355 If we use a Bayes filter as given in (3), keeping X_t and \mathcal{U}_t unchanged whenever $F_t = 0$
 356 introduces new bias. To prevent this, we set $\mathcal{U}_{t+1} = \mathcal{U}_t \cup \partial B$ in step 3.b), effectively deleting
 357 the part of the configuration that was revealed by the filter. Since the algorithm only
 358 terminates once $\mathcal{U}_t = \emptyset$, we further require the Bayes filter correction to ensure that the
 359 probability of $F_t = 0$ is small to guarantee efficiency.

360 Constructing a Bayes filter correction that satisfies the requirements above and allows
 361 for efficient sampling of F_t is a non-trivial task. In the next subsections, we present two
 362 approaches for this, the first specialized to the hard-sphere model without requirements, and
 363 the second one for more general potentials with strong spatial mixing of the point process.
 364 Crucially, assuming strong spatial mixing, both constructions allow us to control the success
 365 probability of the Bayes filter via the update radius ℓ in the construction of the updated set
 366 of boxes B (see step 1).
 367
 368

369 2.1 Bayes filter for the hard-sphere model

370 To construct a Bayes filter for the hard-sphere model, we efficiently approximate the right-
 371 hand side of (4). To approximate the infimum over the uncountable set of configurations
 372 $\xi \in \mathcal{N}_{\Lambda_H}$ we take the minimum over a finite, but sufficiently rich set of configurations,
 373 balancing the quality of approximation with the computation required. In fact the number

38:10 Perfect Sampling for Hard Spheres from Strong Spatial Mixing

374 of configurations needed will depend only on the volume of $\Lambda_{B \cup \partial B}$. We approximate the
 375 fraction of partition functions in (4) with running time only depending on the volume of
 376 $\Lambda_{B \cup \partial B}$. As a result, we efficiently compute a Bayes filter correction $C_\varepsilon(\cdot)$, with the parameter
 377 $\varepsilon > 0$ controlling how much $C_\varepsilon(\mathcal{U}_t, \mathbf{u}_t, X_t)$ deviates from the right-hand side of (4).

378 While our construction of $C_\varepsilon(\cdot)$ guarantees correctness of the sampling algorithm for
 379 any $\varepsilon > 0$, proving efficiency requires more. With strong spatial mixing, we choose ε so
 380 that the probability that $F_t = 0$ is uniformly bounded above, ensuring $O(|\Lambda|)$ iterations in
 381 expectation.

382 It remains to argue that we can efficiently sample F_t , using the Bayes filter correction
 383 $C_\varepsilon(\cdot)$. Explicitly computing the success probability of F_t as in (3) would require computing
 384 the fraction of partition functions on the right-hand side exactly, while approximating these
 385 partition functions would require that the approximation error only depends on $X_t \cap \Lambda_{\mathcal{U}_t}$, to
 386 avoid new bias.

387 It is unclear how to implement these approaches, so instead we use Bernoulli factories to
 388 sample F_t without knowing the success probability. To do so, we observe that the fraction of
 389 partition functions can be written as a ratio of probabilities for drawing the empty set from a
 390 conditional hard-sphere model on Λ_B and $\Lambda_{B \setminus \{\mathbf{u}_t\}}$. Since both regions have constant volume,
 391 rejection sampling obtains Bernoulli random variables with these success probabilities in
 392 constant time. Hence, we obtain a Bernoulli factory for F_t with constant expected running
 393 time. Wald's identity yields a total expected running time $O(|\Lambda|)$ for the algorithm.

394 2.2 Bayes filter for general potentials

395 We now consider the case of general bounded-range, repulsive potentials. Unlike the hard
 396 sphere model, it is not clear here how to approximate the infimum in (4) from a finite set of
 397 boundary configurations. However, given constants $a, b > 0$ such that ϕ satisfies (a, b) -strong
 398 spatial mixing, we can explicitly compute a function $\delta(a, b)$ so that

$$399 \quad C_{a,b}(\mathcal{U}_t, \mathbf{u}_t, X_t) = \delta(a, b) \cdot \frac{Z_{\Lambda_B \setminus \{\mathbf{u}_t\}}(\lambda_{X_t \cap \Lambda_{\mathcal{U}_t}})}{Z_{\Lambda_B}(\lambda_{X_t \cap \Lambda_{\mathcal{U}_t \setminus \{\mathbf{u}_t\}}})}$$

400 is a Bayes filter correction. With strong spatial mixing, we use $C_{a,b}(\cdot)$ to construct a Bayes
 401 filter such that probability that $F_t = 0$ is bounded above, again implying a bound of $O(|\Lambda|)$
 402 on the expected number of iterations of the algorithm.

403 Note that in this setting, we require spatial mixing for both correctness and efficiency,
 404 while for the hard-sphere model we only need it for efficiency. Another crucial difference is
 405 that, while we can explicitly compute $\delta(a, b)$, the same does not hold for $C_{a,b}(\cdot)$ due to the
 406 fraction of partition functions involved. Again we circumvent this by rewriting the success
 407 probability of the Bayes filter in a suitable way and applying a Bernoulli factory for sampling
 408 F_t . Finally, we point out that we do not obtain a constant bound for the expected running
 409 time of each iteration, but instead the bound depends on the number of points in $X_t \cap \Lambda_{\partial B}$.
 410 Possible dependencies between the configuration X_t and the number of iterations prevent us
 411 from bounding the total expected running time using Wald's identity. Instead, we provide
 412 tail bounds on the number of iterations and the running time of each iteration, allowing us to
 413 derive an expected total running time that is linear in the volume of Λ up to polylogarithmic
 414 factors.

3 Preliminaries

Throughout the paper, we write \mathbb{N} for the set of strictly positive integers, and we write $\mathbb{N}_0 = \mathbb{N} \cup \{0\}$. For any $k \in \mathbb{N}$, we denote by $[k]$ the set $[1, k] \cap \mathbb{N}$.

For a bounded measurable region $\Lambda \subset \mathbb{R}^d$ and any finite point configuration $\eta \in \mathcal{N}_\Lambda$, we write $|\eta|$ for the number of points in η . Note that this notation is the same that as the one we use for the volume of a region. The particular meaning will be clear from the context. Moreover, for $k \in \mathbb{N}$, we write $\binom{\eta}{k}$ for the set $\{\eta' \subseteq \eta \mid |\eta'| = k\}$.

3.1 Gibbs point processes

We introduce some additional notation for Gibbs point processes, used in the rest of the paper. Firstly, when dealing with a tuple $(x_1, \dots, x_k) \in (\mathbb{R}^d)^k$ we frequently denote it by the corresponding bold letter \mathbf{x} . Based on this, we write $d\mathbf{x}$ for $dx_1 \dots dx_k$ and $H(\mathbf{x})$ for $H(x_1, \dots, x_k)$. Moreover, for any $k \in \mathbb{N}_0$ and $\mathbf{x} = (x_1, \dots, x_k) \in (\mathbb{R}^d)^k$ we write $\eta_{\mathbf{x}}$ for the set $\{x_1, \dots, x_k\}$, where the case $k = 0$ results in $\eta_{\mathbf{x}} = \emptyset$. Finally, for $\mathbf{x} \in \Lambda^k$ we write $\boldsymbol{\lambda}^{\mathbf{x}}$ for $\prod_{i \in [k]} \boldsymbol{\lambda}(x_i)$. This simplifies the definition of $\mu_{\boldsymbol{\lambda}}$ given in the introduction to

$$\mu_{\boldsymbol{\lambda}}(A) = \frac{1}{Z_\Lambda(\boldsymbol{\lambda})} \sum_{k \geq 0} \frac{1}{k!} \int_{\Lambda^k} \mathbb{1}_{\eta_{\mathbf{x}} \in A} \boldsymbol{\lambda}^{\mathbf{x}} e^{-H(\mathbf{x})} d\mathbf{x}.$$

Next, we formalize two different notions of restricting a Gibbs point process on Λ to a subregion $\Lambda' \subseteq \Lambda$ that are relevant throughout the paper.

The first is based on restricting the support of $\boldsymbol{\lambda}$ by defining a new activity function $\boldsymbol{\lambda} \mathbb{1}_{\Lambda'} : y \mapsto \boldsymbol{\lambda}(y) \cdot \mathbb{1}_{y \in \Lambda'}$ (for constant activity λ , we write $\lambda \mathbb{1}_{\Lambda'} : y \mapsto \lambda \mathbb{1}_{y \in \Lambda'}$). The resulting Gibbs point process is a probability measure on $(\mathcal{N}_{\Lambda'}, \mathfrak{R}_{\Lambda'})$ with

$$\begin{aligned} \mu_{\boldsymbol{\lambda} \mathbb{1}_{\Lambda'}}(A) &= \frac{1}{Z_\Lambda(\boldsymbol{\lambda} \mathbb{1}_{\Lambda'})} \sum_{k \geq 0} \frac{1}{k!} \int_{\Lambda^k} \mathbb{1}_{\eta_{\mathbf{x}} \in A} (\boldsymbol{\lambda} \mathbb{1}_{\Lambda'})^{\mathbf{x}} e^{-H(\mathbf{x})} d\mathbf{x} \\ &= \frac{1}{Z_{\Lambda'}(\boldsymbol{\lambda})} \sum_{k \geq 0} \frac{1}{k!} \int_{\Lambda'^k} \mathbb{1}_{\eta_{\mathbf{x}} \in A} \boldsymbol{\lambda}^{\mathbf{x}} e^{-H(\mathbf{x})} d\mathbf{x} \end{aligned}$$

for all $A \in \mathfrak{R}_{\Lambda'}$. In particular, for $A = \{\eta \in \mathcal{N}_\Lambda \mid \eta \cap (\Lambda')^c > 0\}$, it holds that $\mu_{\boldsymbol{\lambda} \mathbb{1}_{\Lambda'}}(A) = 0$.

The second way of restricting a Gibbs point process $\mu_{\boldsymbol{\lambda}}$ is by projecting it to a measurable subregion $\Lambda' \subseteq \Lambda$. To this end, we write $\mu_{\boldsymbol{\lambda}}[\Lambda']$ for the image measure of $\mu_{\boldsymbol{\lambda}}$ under the map $\mathcal{N}_\Lambda \rightarrow \mathcal{N}_{\Lambda'}$, $\eta \mapsto \eta \cap \Lambda'$. By construction, $\mu_{\boldsymbol{\lambda}}[\Lambda']$ is a probability distribution on $(\mathcal{N}_{\Lambda'}, \mathfrak{R}_{\Lambda'})$ that, for every $A \in \mathfrak{R}_{\Lambda'}$, assigns a probability

$$\mu_{\boldsymbol{\lambda}}[\Lambda'](A) = \frac{1}{Z_\Lambda(\boldsymbol{\lambda})} \sum_{k \geq 0} \frac{1}{k!} \int_{\Lambda^k} \mathbb{1}_{\eta_{\mathbf{x}} \cap \Lambda' \in A} \boldsymbol{\lambda}^{\mathbf{x}} e^{-H(\mathbf{x})} d\mathbf{x}.$$

As discussed in Section 1, we frequently modify the activity function to encode the effect of fixing a certain point set (boundary condition). More precisely, for a fixed potential ϕ , an activity function $\boldsymbol{\lambda}$ and a point set $\eta \in \mathcal{N}_\Lambda$ we write $\boldsymbol{\lambda}_\eta$ for the function $y \mapsto \boldsymbol{\lambda}(y) e^{-\sum_{x \in \eta} \phi(x, y)}$. Similarly, for $k \in \mathbb{N}$ and $\mathbf{x} \in \Lambda^k$ we write $\boldsymbol{\lambda}_{\mathbf{x}}$ for the activity function $y \mapsto \boldsymbol{\lambda}(y) e^{-\sum_{i \in [k]} \phi(x_i, y)}$. We extend this notation to constant activity $\lambda \in \mathbb{R}_{\geq 0}$, writing $\lambda_\eta : y \mapsto \lambda e^{-\sum_{x \in \eta} \phi(x, y)}$ and $\lambda_{\mathbf{x}} : y \mapsto \lambda e^{-\sum_{i \in [k]} \phi(x_i, y)}$. Using this notation, a useful alternative definition of $\mu_{\boldsymbol{\lambda}}[\Lambda']$ is given by

$$\mu_{\boldsymbol{\lambda}}[\Lambda'](A) = \frac{1}{Z_\Lambda(\boldsymbol{\lambda})} \sum_{k \geq 0} \frac{1}{k!} \int_{\Lambda'^k} \mathbb{1}_{\eta_{\mathbf{x}} \in A} \boldsymbol{\lambda}^{\mathbf{x}} e^{-H(\mathbf{x})} Z_\Lambda(\boldsymbol{\lambda}_{\mathbf{x}} \mathbb{1}_{(\Lambda')^c}) d\mathbf{x}$$

$$= \frac{1}{Z_\Lambda(\boldsymbol{\lambda})} \sum_{k \geq 0} \frac{1}{k!} \int_{\Lambda'^k} \mathbb{1}_{\eta_{\mathbf{x}} \in A} \boldsymbol{\lambda}^{\mathbf{x}} e^{-H(\mathbf{x})} Z_{(\Lambda')^c}(\boldsymbol{\lambda}_{\mathbf{x}}) d\mathbf{x}$$

for $A \in \mathfrak{R}_{\Lambda'}$. In particular, note that

$$\mu_{\lambda \mathbb{1}_{\Lambda'}}[\Lambda'](A) = \frac{1}{Z_{\Lambda'}(\boldsymbol{\lambda})} \sum_{k \geq 0} \frac{1}{k!} \int_{\Lambda'^k} \mathbb{1}_{\eta_{\mathbf{x}} \in A} \boldsymbol{\lambda}^{\mathbf{x}} e^{-H(\mathbf{x})} d\mathbf{x}.$$

While $\mu_{\lambda \mathbb{1}_{\Lambda'}}[\Lambda']$ and $\mu_{\lambda \mathbb{1}_{\Lambda'}}$ seem similar, the former is a distribution on $(\mathcal{N}_{\Lambda'}, \mathfrak{R}_{\Lambda'})$ whereas the latter is defined on $(\mathcal{N}_\Lambda, \mathfrak{R}_\Lambda)$.

3.2 Bernoulli factories

In designing our sampling algorithm, it will be useful to consider the following Bernoulli factory problem. We are given access to a sampler for $\text{Ber}(p)$ and for $\text{Ber}(q)$, that is samplers of Bernoulli random variables with parameters p and q respectively, where we further assume $p < q$. We want to sample a random variable $Z \sim \text{Ber}\left(\frac{p}{q}\right)$.

Most work on Bernoulli factories studies their running time in terms of the number of coin flips required. In our setting, the time needed to generate each of these coin flips is random variable. Fortunately, suitable independence assumptions hold in our setting allowing us to prove the following lemma.

► **Lemma 3.1.** *Fix some $p, q \in [0, 1]$ such that $q - p \geq \epsilon$ for some $\epsilon > 0$. Further assume that we have oracle access to a sampler from $\text{Ber}(p)$ and $\text{Ber}(q)$ in the following sense:*

1. every sample from $\text{Ber}(p)$ (resp. $\text{Ber}(q)$) is independent from all previous samples;
2. the expected running time for obtaining a sample from $\text{Ber}(p)$ (resp. $\text{Ber}(q)$), conditioned on previously obtained samples, is uniformly bounded by some $t \in \mathbb{R}_{\geq 0}$.

Then we can sample from $\text{Ber}\left(\frac{p}{q}\right)$ in $O(t\epsilon^{-2})$ expected time.

4 The algorithm

Let $\Lambda = [0, L]^d$ and consider a Gibbs point processes on Λ with uniform activity $\boldsymbol{\lambda}(x) \equiv \lambda$ for some $\lambda \in \mathbb{R}_{>0}$ and repulsive potential ϕ with finite range $r \in \mathbb{R}_{>0}$. Throughout the analysis of our algorithm, it will be useful to focus on configurations $\eta \in \mathcal{N}_\Lambda$ such that $\phi(x, y) < \infty$ for all $\{x, y\} \in \binom{\eta}{2}$, in which case we call η a *feasible configuration*.

Before stating our algorithm, we first formalize how we divide Λ into smaller boxes, following the description given in Section 2. For a r and L as above, let $N = \lceil L/r \rceil$. We set $\mathcal{V} = \{0, \dots, N-1\}^d$ to be the set of box indices and associate each box index $\mathbf{v} = (v_1, \dots, v_d) \in \mathcal{V}$ with the region $\Lambda_{\mathbf{v}} = ([v_1 r, (v_1 + 1)r) \times \dots \times [v_d r, (v_d + 1)r]) \cap \Lambda$. As in Section 2, we extend this notation to sets of box indices $S \subseteq \mathcal{V}$ by setting $\Lambda_S = \bigcup_{\mathbf{v} \in S} \Lambda_{\mathbf{v}}$. Further, recall that, for $\mathbf{v} \in \mathcal{V}$, we write $\mathbb{B}_k(\mathbf{v})$ for the set of boxes $\mathbf{w} \in \mathcal{V}$ with $\|\mathbf{v} - \mathbf{w}\|_\infty < k$. As mentioned earlier, our algorithm tries to update in each step the point configuration on a subset of boxes $B \subseteq \mathcal{V}$. To this end, for $S \subseteq \mathcal{V}$, $\mathbf{v} \in S$, $r \in \mathbb{R}_{>0}$ and $\ell \in \mathbb{N}$, we define

$$B(S, \mathbf{v}, \ell) := \{\mathbf{v}\} \cup (\mathbb{B}_\ell(\mathbf{v}) \setminus S).$$

We refer to the parameter ℓ as the *update radius*. Finally, recall that we write $\partial S = (\bigcup_{\mathbf{v} \in S} \mathbb{B}_1(\mathbf{v})) \setminus S$ for the outer boundary of $S \subseteq \mathcal{V}$.

Whether the algorithm updates the point configuration in iteration t depends on the outcome of a Bernoulli random variable F_t , called the *Bayes filter*. We introduce the following definition.

494 ► **Definition 4.1.** Fix a repulsive potential ϕ of range $r \in \mathbb{R}_{>0}$, an activity $\lambda \in \mathbb{R}_{>0}$ and
 495 some $\ell \in \mathbb{N}$. We call a function $C : 2^{\mathcal{V}} \times \mathcal{V} \times \mathcal{N}_\Lambda \rightarrow [0, 1]$ a Bayes filter correction if, for all
 496 non-empty $S \subseteq \mathcal{V}$ and $\mathbf{v} \in S$, it holds that

- 497 1. $C(S, \mathbf{v}, \cdot)$ is \mathfrak{R}_{Λ_S} -measurable (in particular $C(S, \mathbf{v}, \eta) = C(S, \mathbf{v}, \eta \cap \Lambda_S)$ for all $\eta \in \mathcal{N}_\Lambda$),
 498 2. there is some $\varepsilon > 0$ such that for $B = B(S, \mathbf{v}, \ell)$, $H = (S \cup B)^c$ and all feasible $\eta \in \mathcal{N}_\Lambda$ it
 499 holds that

$$500 \quad \varepsilon \leq C(S, \mathbf{v}, \eta) \leq \inf_{\substack{\xi \in \mathcal{N}_{\Lambda_H} \\ \xi \cup (\eta \cap \Lambda_S) \text{ is feasible}}} \left\{ \frac{Z_{\Lambda_{B \setminus \{\mathbf{v}\}}}(\lambda_{\xi \cup (\eta \cap \Lambda_S)})}{Z_{\Lambda_B}(\lambda_{\xi \cup (\eta \cap \Lambda_S \setminus \{\mathbf{v}\})})} \right\}.$$

Our perfect sampling procedure is stated in Algorithm 1.

■ **Algorithm 1** Perfect sampling algorithm for repulsive Gibbs point processes

Data: region $\Lambda = [0, L]^d$, repulsive potential ϕ of range at most $r \in \mathbb{R}_{>0}$, activity
 $\lambda \in \mathbb{R}_{>0}$, update radius $\ell \in \mathbb{N}$

1 set $t = 0$, $\mathcal{U}_t = \mathcal{V}$, $X_t = \emptyset$
 2 **while** $\mathcal{U}_t \neq \emptyset$ **do**
 3 draw $\mathbf{u}_t \in \mathcal{U}_t$ uniformly at random
 4 set $B = B(\mathcal{U}_t, \mathbf{u}_t, \ell)$
 5 draw F_t from $\text{Ber}\left(C(\mathcal{U}_t, \mathbf{u}_t, X_t) \cdot \frac{Z_{\Lambda_B}(\lambda_{X_t \cap \Lambda_{\partial B}})}{Z_{\Lambda_{B \setminus \{\mathbf{u}_t\}}}(\lambda_{X_t \cap \Lambda_{\partial B \cup \{\mathbf{u}_t\}})}\right)$ where C is a Bayes
 filter correction as in Definition 4.1
 6 **if** $F_t = 1$ **then**
 7 draw Y from $\mu_{\lambda_{X_t \cap (\Lambda_B)^c}} \mathbb{1}_{\Lambda_B}[\Lambda_B]$
 8 set $X_{t+1} = (X_t \setminus \Lambda_B) \cup Y$
 9 set $\mathcal{U}_{t+1} = \mathcal{U}_t \setminus \{\mathbf{u}_t\}$
 10 **else**
 11 set $\mathcal{U}_{t+1} = \mathcal{U}_t \cup \partial B$
 12 increase t by 1
 13 **return** X_t

501 Before we get to the question of how to sample an appropriate Bayes filter in step 5, the
 502 following statement ensures that the algorithm produces the correct output distribution.
 503

504 ► **Theorem 4.2.** Let $T = \inf_{t \in \mathbb{N}} \{\mathcal{U}_t = \emptyset\}$. Then T is almost surely finite and for all $t \in \mathbb{N}_0$
 505 with $\mathbb{P}[t \geq T] > 0$ and all $A \in \mathfrak{R}_\Lambda$, it holds that $\mathbb{P}[X_t \in A \mid t \geq T] = \mu_\lambda(A)$.

506 We proceed to exemplify how we use Bernoulli factories to sample the Bayes filter. For
 507 brevity, we focus on the hard-sphere model here. The more general case of bounded-range
 508 repulsive potential can be found in the full version of the paper [3].

509 Bayes filter for the hard-sphere model

510 Recall that for the hard-sphere model, we have $\phi(x, y) = \infty$ if $\text{dist}(x, y) < r$ and 0 otherwise.
 511 Given a non-empty set of boxes $S \subseteq \mathcal{V}$, $\mathbf{v} \in S$ and a feasible configuration $\eta \in \mathcal{N}_\Lambda$, we want
 512 to construct a Bayes filter correction $C(S, \mathbf{v}, \eta)$ that allows us to efficiently sample the filter.

513 To this end, set $B = B(S, \mathbf{v}, \ell)$ and $H = (S \cup B)^c$. Our construction makes use of two
 514 ingredients. Firstly, we argue that, instead of minimization over the uncountable set of

38:14 Perfect Sampling for Hard Spheres from Strong Spatial Mixing

515 boundary conditions \mathcal{N}_{Λ_H} , it suffices to minimize over subsets of the finite set $(\delta_1 \mathbb{Z})^d \cap \Lambda_{H \cap \partial B}$
 516 for a sufficiently small $\delta_1 > 0$. Secondly, choosing a sufficiently small $\delta_2 > 0$, we show that
 517 we can approximate the involved partition functions using the function

$$518 \quad \hat{Z}(S, \eta, \delta_2) = \sum_{\gamma \subseteq (\delta_2 \mathbb{Z})^d \cap \Lambda_S} \lambda^{|\gamma|} \delta_2^{|\gamma|} \cdot D(\gamma) \cdot D(\gamma \mid \eta \cap \Lambda_{\partial S}), \quad (5)$$

519 where $D(\gamma) = \prod_{\{x,y\} \in \binom{\gamma}{2}} \mathbb{1}_{\text{dist}(x,y) \geq r}$ and $D(\gamma \mid \eta) = \prod_{x \in \gamma} \prod_{y \in \eta} \mathbb{1}_{\text{dist}(x,y) \geq r}$.

520 The following lemma then gives a way to construct a Bayes filter correction for the
 521 hard-sphere model.
 522

523 ► **Lemma 4.3.** *For non-empty $S \subseteq \mathcal{V}$, $\mathbf{v} \in S$, feasible $\eta \in \mathcal{N}_\Lambda$ and $\varepsilon, \delta_1, \delta_2 > 0$ define*

$$524 \quad C_\varepsilon(S, \mathbf{v}, \eta) := e^{-\varepsilon} \cdot \min_{\gamma \subseteq (\delta_1 \mathbb{Z})^d \cap \Lambda_{H \cap \partial B}} \frac{\hat{Z}(B \setminus \{\mathbf{v}\}, \gamma \cup (\eta \cap \Lambda_S), \delta_2)}{\hat{Z}(B, \gamma \cup (\eta \cap \Lambda_{S \setminus \{\mathbf{v}\}}), \delta_2)},$$

525 where $B = B(S, \mathbf{v}, \ell)$ and $H = (S \cup B)^c$. For δ_1, δ_2 sufficiently small, depending only on
 526 d, r, ℓ and ε , it holds that $C_\varepsilon(S, \mathbf{v}, \eta)$ is a Bayes filter correction.

527 In fact, we will not use C_ε directly for our Bayes filter, but a slightly scaled version
 528 $0 < e^{-\varepsilon} C_\varepsilon$, which is again a Bayes filter correction. The additional slack allows us to
 529 efficiently sample the Bayes filter by using a Bernoulli factory, as we argue in the next lemma.
 530

531 ► **Lemma 4.4.** *Let $S \subseteq \mathcal{V}$ be non-empty, $\mathbf{v} \in S$ and $\eta \in \mathcal{N}_\Lambda$ be feasible, and set $B = B(S, \mathbf{v}, \ell)$.
 532 For all $\varepsilon > 0$ we can sample a Bernoulli random variable with success probability*

$$533 \quad e^{-\varepsilon} C_\varepsilon(S, \mathbf{v}, \eta) \cdot \frac{Z_{\Lambda_B}(\lambda_{\eta \cap \Lambda_{\partial B}})}{Z_{\Lambda_{B \setminus \{\mathbf{v}\}}}(\lambda_{\eta \cap \Lambda_{\partial B \cup \{\mathbf{v}\}}})}$$

534 with expected running time only depending on $\varepsilon, \ell, r, \lambda$ and d .

535 The core idea of the above lemma to express $\frac{Z_{\Lambda_B}(\lambda_{\eta \cap \Lambda_{\partial B}})}{Z_{\Lambda_{B \setminus \{\mathbf{v}\}}}(\lambda_{\eta \cap \Lambda_{\partial B \cup \{\mathbf{v}\}}})}$ as a fraction of probabilities.

536 Together with the fact that $e^{-\varepsilon} C_\varepsilon(S, \mathbf{v}, \eta) < 1$, this allows us to write the success probability
 537 of the Bayes filter as a fraction of probabilities $\frac{p}{q}$. Arguing that $p < q$, and that we can
 538 sample $\text{Ber}(p)$ and $\text{Ber}(q)$ efficiently allows us to apply Lemma 3.1 to prove Lemma 4.4.

539 While the above suffices to perform each iteration of Algorithm 1 efficiently, we still
 540 need to bound the number of iterations. For this, we derive a lower bound on the success
 541 probability of the Bayes filter with correction $e^{-\varepsilon} C_\varepsilon(\cdot)$ for a particular choice of ε , using the
 542 assumption of strong spatial mixing.

543 ► **Lemma 4.5.** *Consider a hard-sphere model that exhibits (a, b) -strong spatial mixing up
 544 to λ . Then there are constants a', b' , only depending on a, b, r, λ and d , such that for all
 545 non-empty $S \subseteq \mathcal{V}$, $\mathbf{v} \in S$ and feasible $\eta \in \mathcal{N}_\Lambda$ it holds that*

$$546 \quad e^{-e^{-\ell}} C_{e^{-\ell}}(S, \mathbf{v}, \eta) \cdot \frac{Z_{\Lambda_B}(\lambda_{\eta \cap \Lambda_{\partial B}})}{Z_{\Lambda_{B \setminus \{\mathbf{v}\}}}(\lambda_{\eta \cap \Lambda_{\partial B \cup \{\mathbf{v}\}}})} \geq 1 - a' e^{-b' \ell}.$$

547 Lemma 4.5 allows us to control the success probability of the Bayes filter in terms of ℓ .
 548 Combining the results above gives the following theorem.

549 ► **Theorem 4.6.** *Consider Algorithm 1 on a hard-sphere model with $C(\cdot) = e^{-e^{-\ell}} C_{e^{-\ell}}(\cdot)$ as
 550 Bayes filter correction in line 5. We can run the algorithm in almost-surely finite running
 551 time and, on termination, it outputs a sample from the hard-sphere Gibbs measure μ_λ on Λ .
 552 Moreover, if the hard-sphere model satisfies (a, b) -strong spatial mixing and if ℓ is chosen as
 553 a sufficiently large constant, depending on a, b, r, λ and d , then we can run the algorithm in
 554 expected time $O(|\Lambda|)$.*

555 — References —

- 556 1 Michael Aizenman and Richard Holley. Rapid convergence to equilibrium of stochastic Ising
557 models in the Dobrushin Shlosman regime. *Percolation theory and ergodic theory of infinite*
558 *particle systems*, pages 1–11, 1987.
- 559 2 Berni Julian Alder and Thomas Everett Wainwright. Phase transition for a hard sphere system.
560 *The Journal of Chemical Physics*, 27(5):1208–1209, 1957.
- 561 3 Konrad Anand, Andreas Göbel, Marcus Pappik, and Will Perkins. Perfect sampling for hard
562 spheres from strong spatial mixing. *arXiv preprint arXiv:2305.02450*, 2023.
- 563 4 Konrad Anand and Mark Jerrum. Perfect sampling in infinite spin systems via strong spatial
564 mixing. *SIAM Journal on Computing*, 51(4):1280–1295, 2022.
- 565 5 Søren Asmussen, Peter W Glynn, and Hermann Thorisson. Stationarity detection in the initial
566 transient problem. *ACM Transactions on Modeling and Computer Simulation (TOMACS)*,
567 2(2):130–157, 1992.
- 568 6 Etienne P Bernard and Werner Krauth. Two-step melting in two dimensions: first-order
569 liquid-hexatic transition. *Physical Review Letters*, 107(15):155704, 2011.
- 570 7 Etienne P Bernard, Werner Krauth, and David B Wilson. Event-chain Monte Carlo algorithms
571 for hard-sphere systems. *Physical Review E*, 80(5):056704, 2009.
- 572 8 Steffen Betsch and Günter Last. On the uniqueness of Gibbs distributions with a non-negative
573 and subcritical pair potential. In *Annales de l’Institut Henri Poincaré (B) Probabilités et*
574 *statistiques*, volume 59, pages 706–725. Institut Henri Poincaré, 2023.
- 575 9 Siddharth Bhandari and Sayantan Chakraborty. Improved bounds for perfect sampling of
576 k-colorings in graphs. In *Proceedings of the 52nd Annual ACM SIGACT Symposium on Theory*
577 *of Computing*, pages 631–642, 2020.
- 578 10 Zongchen Chen, Kuikui Liu, Nitya Mani, and Ankur Moitra. Strong spatial mixing for colorings
579 on trees and its algorithmic applications. *arXiv preprint arXiv:2304.01954*, 2023.
- 580 11 Hofer Temmel Christoph. Disagreement percolation for the hard-sphere model. *Electronic*
581 *Journal of Probability*, 24:1–22, 2019.
- 582 12 David Dereudre. Introduction to the theory of Gibbs point processes. In *Stochastic Geometry*,
583 pages 181–229. Springer, 2019.
- 584 13 Persi Diaconis. The Markov Chain Monte Carlo revolution. *Bulletin of the American*
585 *Mathematical Society*, 46(2):179–205, 2009.
- 586 14 Shaddin Dughmi, Jason Hartline, Robert D Kleinberg, and Rad Niazadeh. Bernoulli factories
587 and black-box reductions in mechanism design. *Journal of the ACM (JACM)*, 68(2):1–30,
588 2021.
- 589 15 Martin Dyer, Alistair Sinclair, Eric Vigoda, and Dror Weitz. Mixing in time and space for
590 lattice spin systems: A combinatorial view. *Random Structures & Algorithms*, 24(4):461–479,
591 2004.
- 592 16 Michael Engel, Joshua A Anderson, Sharon C Glotzer, Masaharu Isobe, Etienne P Bernard,
593 and Werner Krauth. Hard-disk equation of state: First-order liquid-hexatic transition in two
594 dimensions with three simulation methods. *Physical Review E*, 87(4):042134, 2013.
- 595 17 Stefan Felsner and Lorenz Wernisch. Markov chains for linear extensions, the two-dimensional
596 case. In *SODA*, pages 239–247, 1997.
- 597 18 Weiming Feng, Heng Guo, and Yitong Yin. Perfect sampling from spatial mixing. *Random*
598 *Structures & Algorithms*, 61(4):678–709, 2022.
- 599 19 Weiming Feng and Yitong Yin. On local distributed sampling and counting. In *Proceedings of*
600 *the 2018 ACM Symposium on Principles of Distributed Computing*, pages 189–198, 2018.
- 601 20 Roberto Fernández, Aldo Procacci, and Benedetto Scoppola. The analyticity region of the
602 hard sphere gas. Improved bounds. *J. Stat. Phys.*, 5:1139–1143, 2007.
- 603 21 Pablo A Ferrari, Roberto Fernández, and Nancy L Garcia. Perfect simulation for interacting
604 point processes, loss networks and Ising models. *Stochastic Processes and their Applications*,
605 102(1):63–88, 2002.

- 606 22 David Gamarnik, Dmitriy Katz, and Sidhant Misra. Strong spatial mixing of list coloring of
607 graphs. *Random Structures & Algorithms*, 46(4):599–613, 2015.
- 608 23 Nancy L Garcia. Perfect simulation of spatial processes. *Resenhas do Instituto de Matemática
609 e Estatística da Universidade de São Paulo*, 4(3):283–325, 2000.
- 610 24 J Groeneveld. Two theorems on classical many-particle systems. *Phys. Letters*, 3, 1962.
- 611 25 Heng Guo and Mark Jerrum. Perfect simulation of the hard disks model by partial rejection
612 sampling. *Annales de l’Institut Henri Poincaré D*, 8(2):159–177, 2021.
- 613 26 Heng Guo, Mark Jerrum, and Jingcheng Liu. Uniform sampling through the Lovász local
614 lemma. *Journal of the ACM (JACM)*, 66(3):1–31, 2019.
- 615 27 Olle Häggström and Karin Nelander. Exact sampling from anti-monotone systems. *Statistica
616 Neerlandica*, 52(3):360–380, 1998.
- 617 28 Olle Häggström, Marie-Colette N.M. van Lieshout, and Jesper Møller. Characterization results
618 and Markov chain Monte Carlo algorithms including exact simulation for some spatial point
619 processes. *Bernoulli*, 5(4):641–658, 1999.
- 620 29 Thomas P Hayes and Cristopher Moore. Lower bounds on the critical density in the hard disk
621 model via optimized metrics. *arXiv preprint arXiv:1407.1930*, 2014.
- 622 30 Kun He, Xiaoming Sun, and Kewen Wu. Perfect sampling for (atomic) Lovász Local Lemma.
623 *arXiv preprint arXiv:2107.03932*, 2021.
- 624 31 Kun He, Chunyang Wang, and Yitong Yin. Sampling Lovász Local Lemma for general
625 constraint satisfaction solutions in near-linear time. In *2022 IEEE 63rd Annual Symposium
626 on Foundations of Computer Science (FOCS)*, pages 147–158. IEEE, 2022.
- 627 32 Kun He, Kewen Wu, and Kuan Yang. Improved bounds for sampling solutions of random CNF
628 formulas. In *Proceedings of the 2023 Annual ACM-SIAM Symposium on Discrete Algorithms
629 (SODA)*, pages 3330–3361. SIAM, 2023.
- 630 33 Tyler Helmuth, Will Perkins, and Samantha Petti. Correlation decay for hard spheres via
631 Markov chains. *The Annals of Applied Probability*, 32(3):2063–2082, 2022.
- 632 34 Christoph Hofer-Temmel and Pierre Houdebert. Disagreement percolation for Gibbs ball
633 models. *Stochastic Processes and their Applications*, 129(10):3922–3940, 2019.
- 634 35 Richard Holley. Possible rates of convergence in finite range, attractive spin systems. *Part.
635 Syst. Random Media Large Deviat.*, 41:215, 1985.
- 636 36 Mark Huber. Spatial birth–death swap chains. *Bernoulli*, 18(3):1031–1041, 2012.
- 637 37 Mark Huber. Nearly optimal Bernoulli factories for linear functions. *Combin. Probab. Comput.*,
638 25(4):577–591, 2016.
- 639 38 Mark Huber, Elise Vilella, Daniel Rozenfeld, and Jason Xu. Bounds on the artificial phase
640 transition for perfect simulation of hard core Gibbs processes. *Involve, a Journal of Mathematics*,
641 5(3):247–255, 2013.
- 642 39 Masaharu Isobe. Hard sphere simulation in statistical physics—methodologies and applications.
643 *Molecular Simulation*, 42(16):1317–1329, 2016.
- 644 40 Vishesh Jain, Ashwin Sah, and Mehtaab Sawhney. Perfectly sampling $k \geq (8/3 + o(1))\Delta$ -
645 colorings in graphs. In *Proceedings of the 53rd Annual ACM SIGACT Symposium on Theory
646 of Computing*, pages 1589–1600, 2021.
- 647 41 Matthew Jenssen, Marcus Michelen, and Mohan Ravichandran. Quasipolynomial-time algo-
648 rithms for repulsive Gibbs point processes. *arXiv preprint arXiv:2209.10453*, 2022.
- 649 42 Mark Jerrum and Alistair Sinclair. The Markov chain Monte Carlo method: an approach to
650 approximate counting and integration. *Approximation algorithms for NP-hard problems*, pages
651 482–520, 1996.
- 652 43 Ravi Kannan, Michael W. Mahoney, and Ravi Montenegro. Rapid mixing of several Markov
653 chains for a hard-core model. In *Algorithms and computation*, volume 2906 of *Lecture Notes
654 in Comput. Sci.*, pages 663–675. Springer, Berlin, 2003.
- 655 44 Frank P Kelly and Brian D Ripley. A note on Strauss’s model for clustering. *Biometrika*,
656 pages 357–360, 1976.

- 657 45 Wilfrid S Kendall. Perfect simulation for the area-interaction point process. In *Probability*
658 *towards 2000*, pages 218–234. Springer, 1998.
- 659 46 Wilfrid S Kendall and Jesper Møller. Perfect simulation using dominating processes on ordered
660 spaces, with application to locally stable point processes. *Advances in Applied Probability*,
661 pages 844–865, 2000.
- 662 47 Botao Li, Yoshihiko Nishikawa, Philipp Höllmer, Louis Carillo, AC Maggs, and Werner Krauth.
663 Hard-disk pressure computations—a historic perspective. *The Journal of Chemical Physics*,
664 157(23):234111, 2022.
- 665 48 Jingcheng Liu, Alistair Sinclair, and Piyush Srivastava. Correlation decay and partition function
666 zeros: Algorithms and phase transitions. *SIAM Journal on Computing*, (0):FOCS19–200,
667 2022.
- 668 49 Laszlo Lovasz and Peter Winkler. Exact mixing in an unknown Markov chain. *The Electronic*
669 *Journal of Combinatorics*, pages R15–R15, 1995.
- 670 50 Hartmut Löwen. Fun with hard spheres. In *Statistical physics and spatial statistics*, volume
671 554, pages 295–331. Springer, 2000.
- 672 51 Pinyan Lu and Yitong Yin. Improved FPTAS for multi-spin systems. In *Approximation, Ran-*
673 *domization, and Combinatorial Optimization. Algorithms and Techniques: 16th International*
674 *Workshop, APPROX 2013, and 17th International Workshop, RANDOM 2013, Berkeley, CA,*
675 *USA, August 21-23, 2013. Proceedings*, pages 639–654. Springer, 2013.
- 676 52 Fabio Martinelli. Lectures on Glauber dynamics for discrete spin models. In *Lectures on*
677 *probability theory and statistics*, pages 93–191. Springer, 1999.
- 678 53 Nicholas Metropolis, Arianna W Rosenbluth, Marshall N Rosenbluth, Augusta H Teller, and
679 Edward Teller. Equation of state calculations by fast computing machines. *The Journal of*
680 *Chemical Physics*, 21(6):1087–1092, 1953.
- 681 54 Marcus Michelen and Will Perkins. Potential-weighted connective constants and uniqueness
682 of Gibbs measures. *arXiv preprint arXiv:2109.01094*, 2021.
- 683 55 Marcus Michelen and Will Perkins. Analyticity for classical gasses via recursion. *Communica-*
684 *tions in Mathematical Physics*, pages 1–22, 2022.
- 685 56 Marcus Michelen and Will Perkins. Strong spatial mixing for repulsive point processes. *Journal*
686 *of Statistical Physics*, 189(1):9, 2022.
- 687 57 Sarat B Moka, Dirk P Kroese, et al. Perfect sampling for Gibbs point processes using partial
688 rejection sampling. *Bernoulli*, 26(3):2082–2104, 2020.
- 689 58 Jesper Møller. A review of perfect simulation in stochastic geometry. *Lecture Notes-Monograph*
690 *Series*, pages 333–355, 2001.
- 691 59 Jesper Møller and Rasmus Plenge Waagepetersen. *Statistical inference and simulation for*
692 *spatial point processes*. CRC Press, 2003.
- 693 60 Duncan J Murdoch and Peter J Green. Exact sampling from a continuous state space.
694 *Scandinavian Journal of Statistics*, 25(3):483–502, 1998.
- 695 61 Serban Nacu and Yuval Peres. Fast simulation of new coins from old. *The Annals of Applied*
696 *Probability*, 15(1A):93–115, 2005.
- 697 62 Oliver Penrose. Convergence of fugacity expansions for fluids and lattice gases. *Journal of*
698 *Mathematical Physics*, 4(10):1312–1320, 1963.
- 699 63 James Gary Propp and David Bruce Wilson. Exact sampling with coupled Markov chains and
700 applications to statistical mechanics. *Random Structures & Algorithms*, 9(1-2):223–252, 1996.
- 701 64 James Gary Propp and David Bruce Wilson. How to get a perfectly random sample from a
702 generic Markov chain and generate a random spanning tree of a directed graph. *Journal of*
703 *Algorithms*, 27(2):170–217, 1998.
- 704 65 Dana Randall. Rapidly mixing Markov chains with applications in computer science and
705 physics. *Computing in Science & Engineering*, 8(2):30–41, 2006.
- 706 66 Guus Regts. Absence of zeros implies strong spatial mixing. *Probability Theory and Related*
707 *Fields*, pages 1–21, 2023.
- 708 67 David Ruelle. Correlation functions of classical gases. *Annals of Physics*, 25:109–120, 1963.

38:18 Perfect Sampling for Hard Spheres from Strong Spatial Mixing

- 709 **68** David Ruelle. *Statistical mechanics: Rigorous results*. World Scientific, 1999.
- 710 **69** Alistair Sinclair, Piyush Srivastava, Daniel Štefankovič, and Yitong Yin. Spatial mixing and the
711 connective constant: Optimal bounds. *Probability Theory and Related Fields*, 168(1-2):153–197,
712 2017.
- 713 **70** Yinon Spinka. Finitary codings for spatial mixing Markov random fields. *Ann. Probab.*,
714 48(3):1557–1591, 2020.
- 715 **71** David J Strauss. A model for clustering. *Biometrika*, 62(2):467–475, 1975.
- 716 **72** Daniel W Stroock and Boguslaw Zegarlinski. The logarithmic Sobolev inequality for discrete
717 spin systems on a lattice. *Communications in Mathematical Physics*, 149(1):175–193, 1992.
- 718 **73** Marie-Colette N.M. van Lieshout. *Markov Point Processes and Their Applications*. 2000.
- 719 **74** Dror Weitz. Counting independent sets up to the tree threshold. In *Proceedings of the*
720 *Thirty-Eighth Annual ACM Symposium on Theory of Computing*, STOC 2006, pages 140–149.
721 ACM, 2006.
- 722 **75** William W. Wood, F. Raymond Parker, and Jack David Jacobson. Recent monte carlo
723 calculations of the equation of state of lenard-jones and hard sphere molecules. *Il Nuovo*
724 *Cimento (1955-1965)*, 9:133–143, 1958.